

[Supporting Information]

Hyperconjugation-Induced Chromism in Linear Responsive Polymer

AUTHORS

Yeol Kyo Choi,^{‡a} Sang Yup Lee^{‡b} and Dong June Ahn^{*ab}

AFFILIATIONS

^a Department of Chemical and Biological Engineering, Korea University, Seoul 02841, Republic of Korea

^b KU-KIST Graduate School of Converging Science and Technology, Korea University, Seoul 02841, Republic of Korea

*Corresponding author, E-mail: ahn@korea.ac.kr

[‡] These authors contributed equally to this work

CONTENTS

Materials and Methods

Fig. S1. Coarse-grained model of TCDA and underlying atomistic structure.

Fig. S2. Potential energy scan for backbone moiety in PDA.

Fig. S3. Calculated UV-vis spectra and effective conjugation length of PDAs.

Fig. S4. Crystallographic lattice parameters of monomeric, blue, and red state of PDAs.

Fig. S5. Time-traced extents of hydrogen bonding of PDAs.

Table S1. TCDA CG bonded parameters.

Table S2. AA bonded parameters for backbone structure of PDAs.

Table S3. Structural changes of PDA by thermal stimulation.

Table S4. Second-order perturbation theory analysis of fock matrix in NBO basis for blue and red states of PDAs

Materials and Methods

System Parameters

All molecular dynamics (MD) run were performed with Gromacs 5.1.4⁴⁹⁻⁵¹ using the MARTINI FF⁵² for coarse-grained (CG) MD and CHARMM36 FF⁵³ with additional parameters for all-atom (AA) MD. To control the temperature, v-rescale⁵⁴ thermostat was used. The pressure was maintained at 1 bar using the Berendsen⁵⁵ and Parrinello-Rahman⁵⁶ barostats for the equilibrium and production run, respectively. Neighbor lists were built using the Verlet cut-off scheme with a cut-off radius of 1.2 nm and updated at each step. The linear constraint solver (LINCS)^{57,58} algorithm was used to constrain the bond lengths. All simulations were conducted using a leap-frog integrator with time-steps of 20 and 2 fs for CG and AA MD respectively. Electrostatic interactions were calculated using particle mesh Ewald⁵⁹ with a cutoff of 1.2 nm in AA-MD.

Coarse-grained Simulations

Diacetylene (DA) monomer was parameterized based on previously reported force field parameters⁶⁰. The DA molecule was described by eight beads and one virtual site, one bead for the head group and the others for alkyl chain (Fig. S1). In the experiments, TCDA is self-assembled in a tilted lamella structure. To implement this tilted structure, a different force field in which the bead size is reduced by 10% were used in the alkyl chain⁶¹. The bonded parameters of the CG model were fitted based on the AA model (Table S1). The self-assembly simulation began with random distribution of 288 DA monomers in 2314 CG waters at 343 K for 1 μ s. After equilibrium, the self-assembled structure was cooled to 277 K and further equilibration was performed for 1 μ s based on experimental process. The final CG configuration was retrieved to atomistic resolution by employing a published backmapping protocol³⁷.

Atomistic Simulations

All-atom (AA) models based on the CHARMM36 force field and additional parameters for backbone of PDAs were obtained from QM/MM calculations (see Table S2). Well-ordered single crystal DA bilayer was reconstructed from the stabilized structure by backmapping and was polymerized upon topochemical criteria. This polymerized bilayer consisting of 24 polymer chains with 12-mer length was connected via periodic boundary condition to form infinite polymer and used for all analysis. In the reversibility analysis (see main text), each temperature state in the thermal cycle (298→373 →298 K) was simulated for 50 ns, respectively. The relative energies of blue and red state in Fig. 4C were calculated from summation of bonded and nonbonded energies in the hyperconjugation region and side-chain of PDAs chain. The hydrogen bonding was calculated using HBOND tool in GROMACS.

Quantum Mechanical Computations

Initial geometries of the 12-mer long PDAs containing only C_α and C_β were extracted in AA-MD results for blue and red states, respectively. The ground-state geometries were optimized with Gaussian 09 software⁶² using the DFT/B3LYP⁶³ functional and 6-311G(d,p) basis set with constraint on dihedral angle, $C_\beta-C_\alpha-C_1=C'_4$ for both cases. The natural bonding orbitals' (NBO) calculations were performed using NBO 3.1 program⁶⁴ implemented in the Gaussian 09 package at the DFT/B3LYP/6-311G(d,p) level for each state. The vibrational frequencies were also done using DFT/B3LYP functional and 6-311G(d,p) basis set. Then the twenty lowest singlet and triplet excited states were calculated by the TD-DFT method at their optimized ground-state geometries using the M06-2X⁶⁵ functional and Def2-TZVP basis set.

Theoretical Colorimetric Response

To quantify the extent of blue and red states in the theoretical analysis, the colorimetric response values (%CR) were calculated based on the equation, $\%CR = [(PB_0 - PB)/PB_0] \times 100$. The PB values were calculated from $PB = A_{170}/(A_{120} + A_{170})$, where A_{170} (blue) and A_{120} (red) were the area of dihedral distribution fitted with Gaussian function at 170° and 120° , corresponding to the amount of blue and red states. The PB_0 and PB represent before and after exposure to external stimuli, respectively.

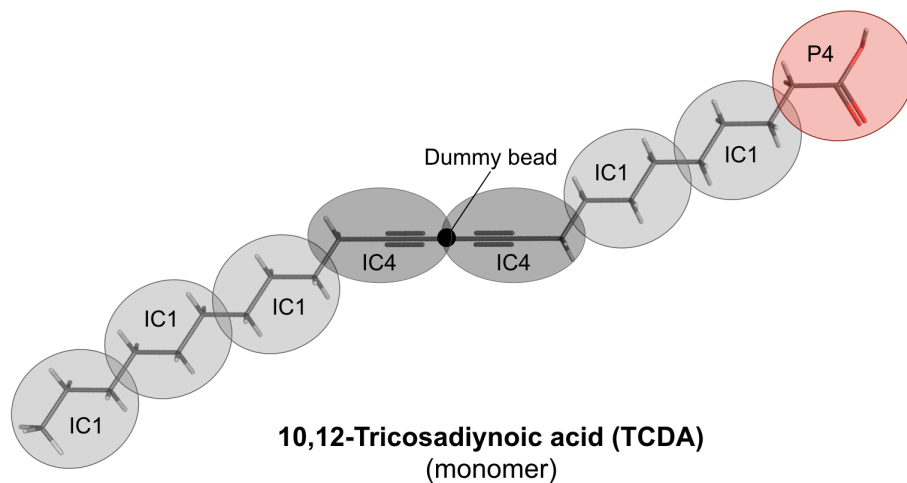


Fig. S1 Coarse-grained model of TCDA and underlying atomistic structure.

Table S1		TCDA CG bonded parameters.	
	Bead types	b_0 (nm)	k_b (kJ mol ⁻¹ nm ⁻²)
bond 1	P4-IC1	0.47	1250
bond 2	IC1-IC1	0.36	4500
bond 3	IC1-IC4	0.36	4500
bond 4	IC4-IC4	0.62	constraints
		θ_0 (degree)	k_θ (kJ mol ⁻¹)
angle 1	P4-IC1-IC1	180	25
angle 2	IC1-IC1-IC1	180	25
angle 3	IC1-IC1-IC4	180	25
angle 4	IC1-IC4-IC4	140	25

Table S2 AA bonded parameters for backbone structure of PDAs

atom types		b_0 (nm)	k_b (kJ mol ⁻¹ nm ⁻²)		
bond 1	CG1T1-CG321 (\equiv C-C-)	0.1465	343088.0		
bond 2	CG1T1-CG1T1 (\equiv C-C \equiv , -C \equiv C-)	0.1120	803328.0		
bond 3	CG2DC1-CG1T1 (=C-C \equiv)	0.1435	288696.0		
bond 4	CG2DC1-CG321 (=C-C-)	0.1502	305432.0		
bond 5	CG2DC1-CG2DC1 (-C=C-)	0.1340	368192.0		
		θ_0 (degree)	k_θ (kJ mol ⁻¹)		
angle 1	CG1T1-CG1T1-CG2DC1 (-C \equiv C-C=)	180.0	158.992		
angle 2	CG1T1-CG1T1-CG321 (-C \equiv C-C-)	180.0	158.992		
angle 3	CG1T1-CG2DC1-CG2DC1 (-C \equiv C-C=)	123.5	401.664		
angle 4	CG1T1-CG2DC1-CG321 (-C \equiv C-C-)	123.5	401.664		
		ϕ_0 (degree)	k_ϕ (kJ mol ⁻¹)	n	
dihedral 1	CG1T1-CG2DC1-CG2DC1-CG1T1	180.0	1.8828	1	
	(\equiv C-C=C-C \equiv)	180.0	35.3564	2	
dihedral 2	CG1T1-CG2DC1-CG2DC1-CG321	180.0	1.8828	1	
	(\equiv C-C=C-C-)	180.0	35.3564	2	
dihedral 3	CG1T1-CG2DC1-CG321-CG321	0.0	0.79496	3	
	(\equiv C-C-C-C-)				
dihedral 4	CG1T1-CG2DC1-CG321-HGA2	0.0	0.79496	3	
	(\equiv C-C-C-H)				
dihedral 5	CG2DC1-CG2DC1-CG321-CG321	180.0	1.2600	1	
	(-C=C-C-C-)	0.0	0.6300	2	
		0.0	0.3800	3	
dihedral 6	CG2DC1-CG2DC1-CG2DC1-CG2DC1	180.0	1.4000	2	
	(-C=C~C=C-)				

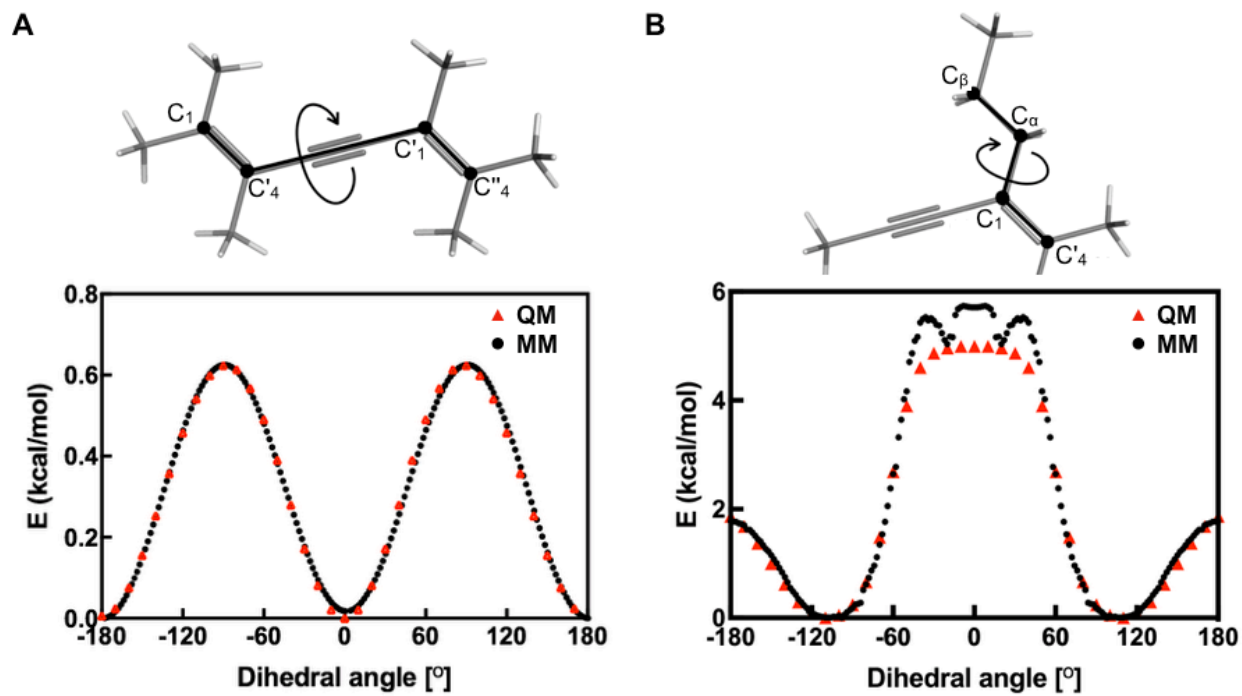


Fig. S2 Potential energy scan of backbone moiety in PDA. (A) $C_1-C'_4-C'_1-C'_4$ and (B) $C_\beta-C_\alpha-C_1-C'_4$ dihedral angles.

Table S3. Structural changes of PDA by thermal stimulation.

	Blue State		Red State	
	Simulation	Experiment ^a	Simulation	Experiment ^a
Bilayer thickness (nm)	4.25	4.3	5.35	5.3
Mean molecular area (Å ²)	24.4	24	20.3	20
Tilt angle (°)	35	37	3	5
Unit cell parameters	a (Å)	4.9	4.9	4.9
	b (Å)	10.0	7.6	7.8
	γ (°)	90	86	84

^aThe experimental results obtained from AFM and GIXD analyses^{30,44}.

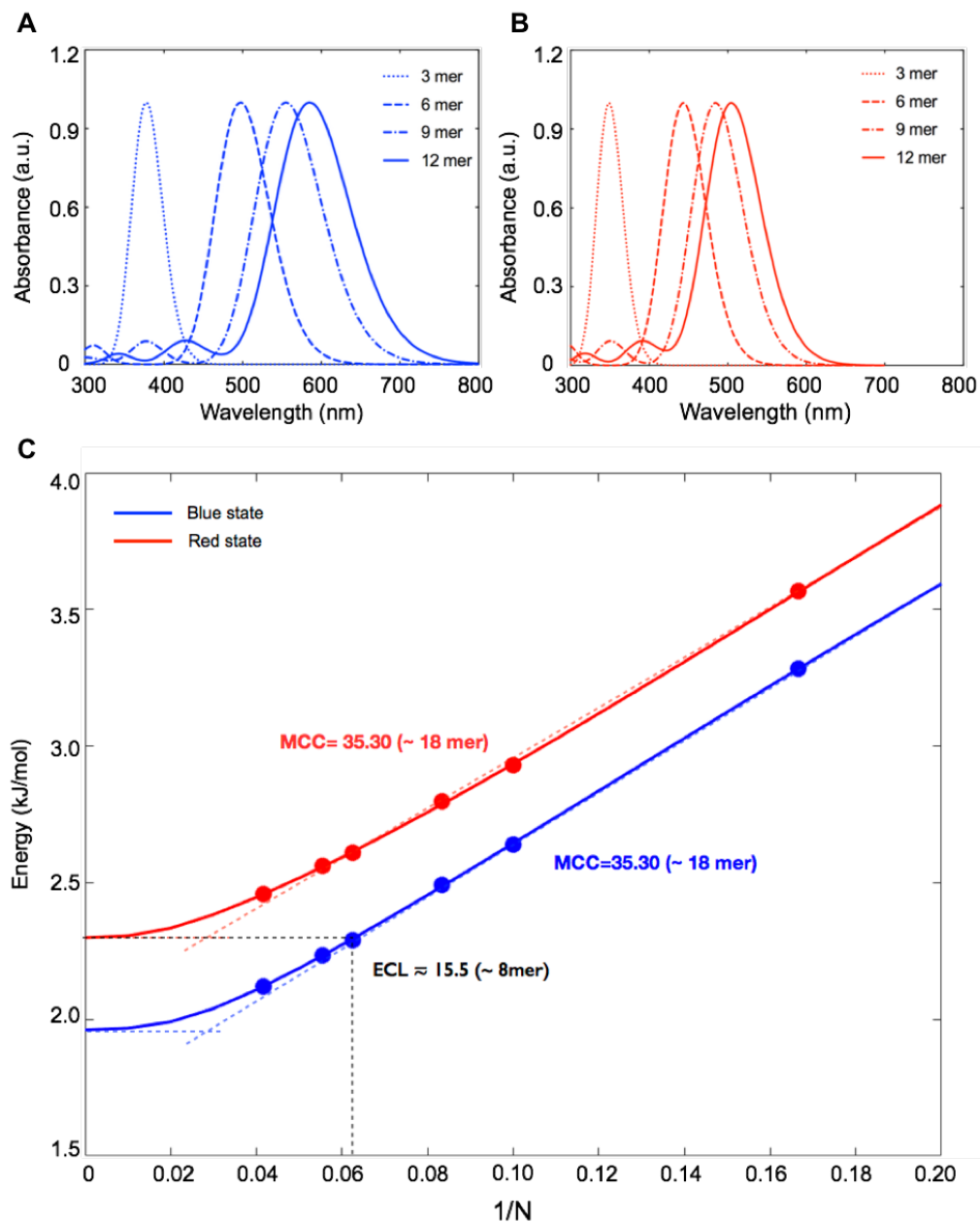


Fig. S3 Calculated UV-vis spectra and effective conjugation length of PDAs. (A) calculated absorption spectra of DAs oligomers and polymer in blue and red states. (B) Vertical (Evert) transition energies of blue and red states PDAs as a function of $1/N$ (closed circle). Solid lines are modified Kuhn fits to the calculated values. The effective conjugation length (ECL) of red state was extracted by graphical method based on the concept of maximum conductive chain length (MCC).

Table S4 Second-order perturbation theory analysis of fock matrix in NBO basis for blue and red states of PDAs.

Donor ^a	Type	Acceptor ^a	Type	E(2) ^b (kJ/mol)	
				Blue state	Red state
C ₁ =C' ₄	π	C ₂ ≡C ₃	π^*	78.53	74.14
		C' ₂ ≡C' ₃	π^*	78.58	74.14
		C _{α} -C _{β}	σ^*	0	11.63
		C' _{α} -C' _{β}	σ^*	0	11.63
		C _{α} -H _{α1}	σ^*	8.83	8.49
		C' _{α} -H' _{α1}	σ^*	8.58	8.54
		C _{α} -H _{α2}	σ^*	8.62	0
		C' _{α} -H' _{α2}	σ^*	8.74	0

^a Atom names described in Fig. 2b.

^b E(2) means energy of hyper conjugative interaction (stabilization energy)

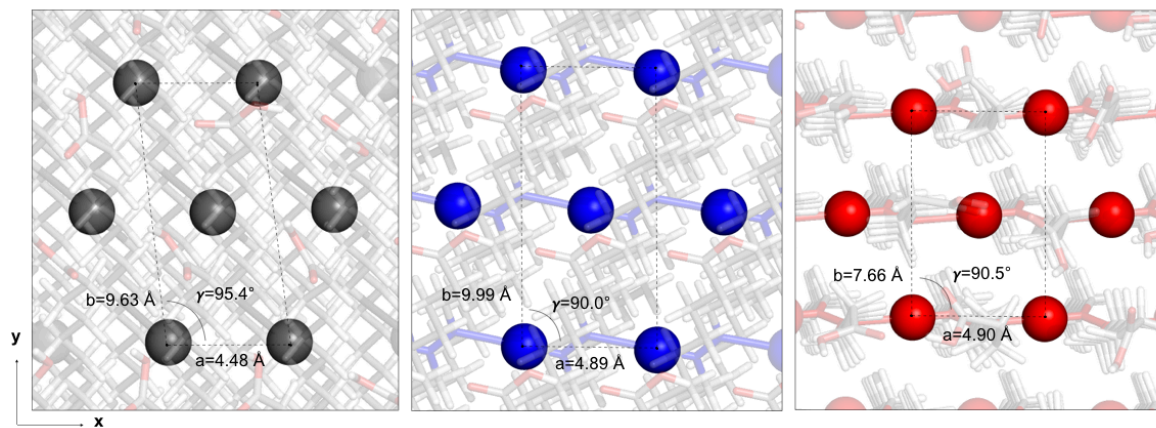


Fig. S4 Crystallographic lattice parameters of monomeric, blue, and red state of PDAs. The a and b axes correspond to the centered cell for each structure. For blue and red states, x-axis direction is defined along the conjugated direction of the polymer. The structural information for each state is summarized in Table S3.

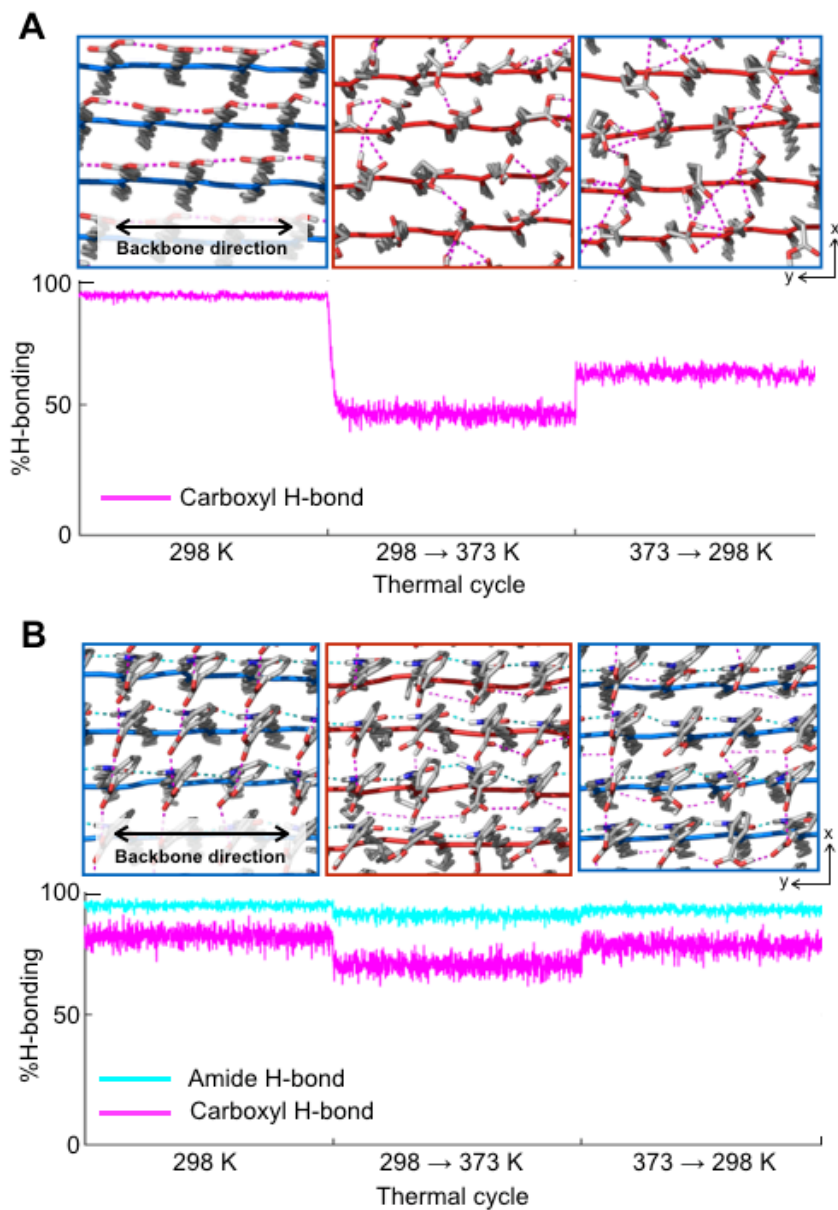


Fig. S5 Time-traced extents of hydrogen bonding for *p*-TCDA (A) and *p*-TCDA-mBzA (B). Top-view images of H-bond network upon the thermal cycle (top panel) and corresponding extent of H-bonds. The carboxyl and amide H-bonds were colored with magenta and cyan dotted lines, respectively.

REFERENCE

49. E. Lindahl, B. Hess and D. Van Der Spoel, *J. Mol. Model.*, 2001, **7**, 306-317.
50. D. Van Der Spoel, E. Lindahl, B. Hess, G. Groenhof, A. E. Mark and H. J. Berendsen, *J. Comput. Chem.*, 2005, **26**, 1701-1718.
51. B. Hess, C. Kutzner, D. Van Der Spoel and E. Lindahl, *J. Chem Theory Comput.*, 2008, **4**, 435-447.
52. S. J. Marrink, H. J. Risselada, S. Yefimov, D. P. Tieleman and A. H. De Vries, *J. Phys. Chem.B*, 2007, **111**, 7812-7824.
53. K. Vanommeslaeghe, E. Hatcher, C. Acharya, S. Kundu, S. Zhong, J. Shim, E. Darian, O. Guvench, P. Lopes and I. Vorobyov, *J. Comput. Chem.*, 2010, **31**, 671-690.
54. G. Bussi, D. Donadio and M. Parrinello, *The J. Chem. Phys.*, 2007, **126**, 014101.
55. H. J. Berendsen, J. v. Postma, W. F. van Gunsteren, A. DiNola and J. Haak, *J. Chem. Phys.*, 1984, **81**, 3684-3690.
56. M. Parrinello and A. Rahman, *J. Appl. Phys.*, 1981, **52**, 7182-7190.
57. B. Hess, H. Bekker, H. J. Berendsen and J. G. Fraaije *J. Comput. Chem.*, 1997, **18**, 1463-1472.
58. B. Hess, *J. Chem. Theory Comput.*, 2008, **4**, 116-122.
59. T. Darden, D. York and L. Pedersen, *J. Chem. Phys.*, 1993, **98**, 10089-10092.
60. M. J. Chun, Y. K. Choi and D. J. Ahn, *RSC Advances*, 2018, **8**, 27988-27994.
61. S. J. Marrink, J. Risselada and A. E. Mark, *Chem. Phys. Lipids*, 2005, **135**, 223-244.
62. M. Frisch, G. Trucks, H. B. Schlegel, G. E. Scuseria, M. A. Robb, J. R. Cheeseman, G. Scalmani, V. Barone, B. Mennucci and G. Petersson, *Inc., Wallingford, CT*, 2009, **200**.
63. A. D. Becke, *J. Chem. Phys.*, 1993, **98**, 5648-5652.
64. E. Glendening, J. Badenhoop, A. Reed, J. Carpenter and F. Weinhold, *University of Wisconsin, Copyright*, 1996, **2001**.
65. Y. Zhao and D. G. Truhlar, *Theor. Chem. Acc.*, 2008, **120**, 215-241.